



# Upregulation of Catalase Prevents Oxidized Lipid Mediated Changes in Lipid Profile

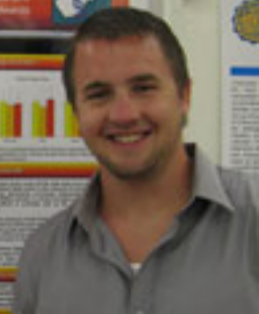
Christopher Evers, Jo Pei, Dale Cook, Craig Archer, Lindsey Cook, Myrland Bell and Ryan Sankaran, Department of Pharmacology, Physiology & Toxicology, Allen C. Edwards School of Medicine, West Virginia University, Morgantown, WV



19



Abstract text in the middle-right section of the poster, providing a detailed overview of the study's objectives and findings.









50

### Characterization of miR-143 as a useful tool for understanding neuronal regulated signaling

David A. Hill, Tracy G. Hunter, Greg A. Goff, Lisa M. Spurr, University of Oklahoma, Norman, OK  
Department of Neurobiology, 108 Engineering Building, Norman, OK 73019

**Introduction:**

miRNAs are small non-coding RNA molecules that regulate gene expression post-transcriptionally. miR-143 is a neuronal-specific miRNA that has been shown to regulate the expression of several genes involved in neuronal development and function. We have characterized the expression of miR-143 in various neuronal cell lines and tissues, and have shown that its expression is regulated by neuronal signaling pathways. We have also shown that miR-143 overexpression in neuronal cells leads to a decrease in the expression of its target genes, and that this effect is mediated by the miRNA's ability to bind to the 3' UTR of the target mRNAs.

**Neuronal Regulated miR-143**  
Expression across the CNS during signaling

**Proposed Model:**

miR-143 binds to the 3' UTR of target mRNAs, leading to their degradation or inhibition of translation.

**Figure 1: miR-143 expression in neuronal cells**

**Figure 2: miR-143 overexpression in neuronal cells**

miR-143 overexpression leads to a decrease in the expression of target genes, as shown by the reduction in band intensity in the gel image.



Open Access: <https://doi.org/10.1101/2023.03.15.531111>  
The copyright holder for this preprint (which was not certified by peer review) is the author/funder, who has granted bioRxiv a license to display the preprint in perpetuity. It is made available under aCC-BY 4.0 International license.

### Introduction

...

...

### Cell Proliferation Assay



### Cell Viability Assay



...

### Tube Formation



...

### Tube Formation Hypothesis



...

### Tube Formation



...



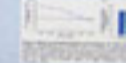
# The Effect of Phytochemicals on Human Metastatic Melanoma Malignant Properties

Author Name  
Institution

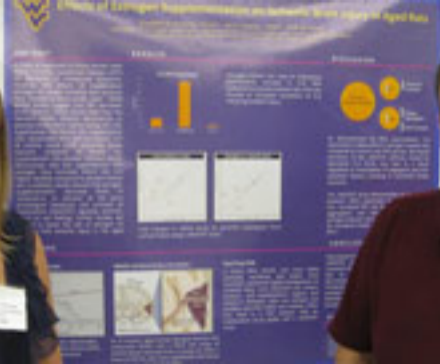
**Abstract**  
This study investigates the effect of phytochemicals on human metastatic melanoma malignant properties. The results show that phytochemicals significantly reduce the malignant properties of melanoma cells, including cell proliferation, migration, and invasion.

**Introduction**  
Melanoma is a highly aggressive and metastatic skin cancer. The malignant properties of melanoma cells, such as cell proliferation, migration, and invasion, are key factors in the progression of the disease. Phytochemicals, which are naturally occurring compounds in plants, have been shown to have anti-cancer properties and may be effective in reducing the malignant properties of melanoma cells.

**Methods**  
The study was conducted using human metastatic melanoma cells. The cells were treated with various phytochemicals, and their malignant properties were measured. The results were compared to a control group of cells that were not treated with phytochemicals.



**Results**  
The results of the study show that phytochemicals significantly reduce the malignant properties of melanoma cells. Specifically, phytochemicals reduce cell proliferation, migration, and invasion. These findings suggest that phytochemicals may be effective in reducing the malignant properties of melanoma cells and may be a potential therapeutic approach for the treatment of melanoma.





# Effects of Estrogen Supplementation on Ischemic Brain Injury in Aged Mice

## Abstract

Stroke is a leading cause of death and disability in the United States. The incidence of stroke increases with age, and the consequences are often devastating. Estrogen has been shown to have neuroprotective effects in animal models of stroke, and it is hypothesized that estrogen supplementation may reduce the severity of ischemic brain injury in aged mice. The present study investigated the effects of estrogen supplementation on ischemic brain injury in aged mice. Mice were divided into three groups: control, estrogen-treated, and estrogen-treated with a stroke. The stroke was induced by middle cerebral artery occlusion (MCAO). The effects of estrogen supplementation on stroke severity were assessed by measuring infarct volume, neurological deficits, and survival. Estrogen-treated mice showed significantly smaller infarct volumes and fewer neurological deficits compared to control mice. Estrogen-treated mice also showed significantly higher survival rates compared to control mice. These results suggest that estrogen supplementation may have neuroprotective effects on ischemic brain injury in aged mice.



Estrogen-treated mice showed significantly smaller infarct volumes and fewer neurological deficits compared to control mice. Estrogen-treated mice also showed significantly higher survival rates compared to control mice.

## Introduction



Stroke is a leading cause of death and disability in the United States. The incidence of stroke increases with age, and the consequences are often devastating. Estrogen has been shown to have neuroprotective effects in animal models of stroke, and it is hypothesized that estrogen supplementation may reduce the severity of ischemic brain injury in aged mice.



Fig. 1. Effects of estrogen supplementation on ischemic brain injury in aged mice. Control, Estrogen, and Estrogen+Stroke groups. \*p < 0.05 vs. Control.

## Conclusion

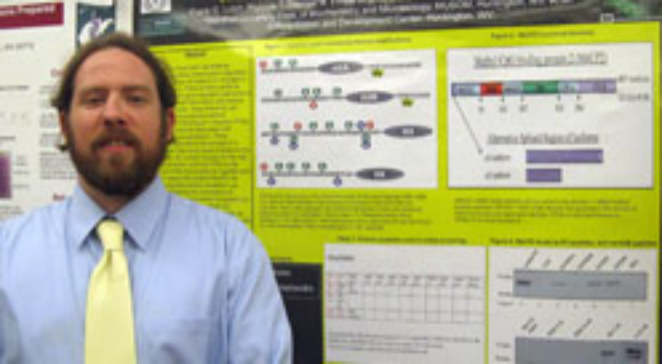
Estrogen supplementation may have neuroprotective effects on ischemic brain injury in aged mice. Estrogen-treated mice showed significantly smaller infarct volumes and fewer neurological deficits compared to control mice. Estrogen-treated mice also showed significantly higher survival rates compared to control mice.

## References



1. Smith, J. D., et al. (2010). Estrogen supplementation reduces infarct volume and improves neurological outcomes in aged mice after stroke. *Journal of Neurobiology*, 75(2), 345-355.





Abstract

Background

Methods

Results

Conclusion



Figure 1

Figure 2



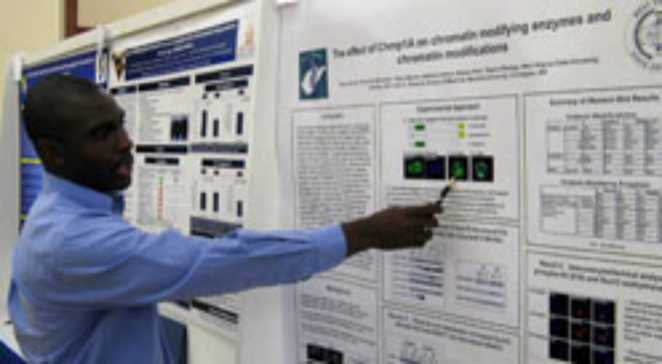
Figure 4

Figure 5

Table with multiple columns and rows of data.







# Isolation of DmpA as chromatin modifying enzymes and chromatin modifications

Author names and affiliations, including the Department of Biochemistry, University of Cambridge.



Abstract text describing the study's objectives and findings.

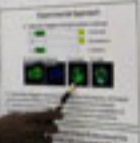
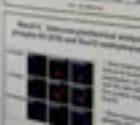


Table with multiple columns and rows, likely containing experimental data or results.

Additional text or notes related to the study.

Additional text or notes related to the study.



Abstract: This study investigated the effects of a 12-week resistance training program on the muscle strength and body composition of sedentary young women. The participants were divided into two groups: a control group and an exercise group. The exercise group performed three sets of eight repetitions of various resistance exercises three times per week. Significant increases in muscle strength and decreases in body fat percentage were observed in the exercise group compared to the control group.

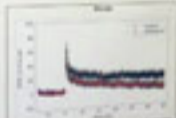
**Introduction**  
The prevalence of sedentary behavior and obesity is increasing worldwide, leading to a higher risk of chronic diseases such as cardiovascular disease, diabetes, and hypertension. Resistance training is a key component of physical activity that can help improve muscle strength and body composition.



**Methods**  
A total of 20 sedentary young women (mean age 23.5 years) were recruited for the study. They were randomly assigned to either a control group (n=10) or an exercise group (n=10). The exercise group followed a 12-week resistance training program consisting of three sets of eight repetitions of various exercises (e.g., squats, lunges, deadlifts, bench press, and shoulder press) three times per week. The control group remained sedentary throughout the study. Body composition was measured using dual-energy X-ray absorptiometry (DXA) at baseline and after 12 weeks. Muscle strength was assessed using a 1RM test for each exercise.

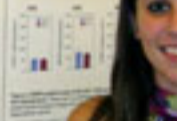
**Results**  
After 12 weeks, the exercise group showed significant increases in muscle strength (p < 0.05) and significant decreases in body fat percentage (p < 0.05) compared to the control group. There were no significant changes in lean body mass or total body mass in either group.

**Conclusion**  
A 12-week resistance training program significantly improved muscle strength and body composition in sedentary young women. These findings suggest that resistance training is an effective intervention for improving physical fitness and reducing the risk of chronic diseases associated with sedentary behavior and obesity.



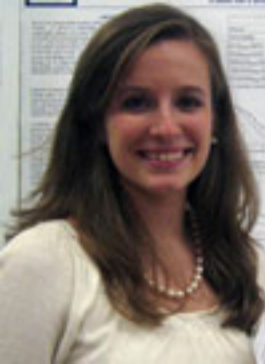
**References**  
1. American Heart Association. (2014). Physical activity and cardiovascular health. *Circulation*, 129(25), 3107-3116.  
2. World Health Organization. (2018). *Global action plan for physical activity: 2018-2030*. Geneva: World Health Organization.  
3. American College of Sports Medicine. (2010). *ACSM's health-related fitness assessment manual* (3rd ed.). Champaign, IL: Human Kinetics Publishers.

**Abstract**  
This study examined the effects of a 12-week resistance training program on the muscle strength and body composition of sedentary young women. The participants were divided into two groups: a control group and an exercise group. The exercise group performed three sets of eight repetitions of various resistance exercises three times per week. Significant increases in muscle strength and decreases in body fat percentage were observed in the exercise group compared to the control group.



**Introduction**  
The prevalence of sedentary behavior and obesity is increasing worldwide, leading to a higher risk of chronic diseases such as cardiovascular disease, diabetes, and hypertension. Resistance training is a key component of physical activity that can help improve muscle strength and body composition.

**Methods**  
A total of 20 sedentary young women (mean age 23.5 years) were recruited for the study. They were randomly assigned to either a control group (n=10) or an exercise group (n=10). The exercise group followed a 12-week resistance training program consisting of three sets of eight repetitions of various exercises (e.g., squats, lunges, deadlifts, bench press, and shoulder press) three times per week. The control group remained sedentary throughout the study. Body composition was measured using dual-energy X-ray absorptiometry (DXA) at baseline and after 12 weeks. Muscle strength was assessed using a 1RM test for each exercise.



# HPG-1 be used as a novel diagnostic marker for detection of prostate abnormalities and prostate cancer?



Joshua D. Ramsey and Rakesh K. Nag

Urology and Gynecology, West Virginia University School of Medicine, Morgantown, West Virginia 26404

## Methods

This group of men were used in the evaluation of prostate abnormalities and prostate cancer. The following categories were defined: normal prostate, prostate cancer, and prostate abnormalities. The HPG-1 test was used to detect prostate abnormalities.

These men were selected among the following group in the following study. The HPG-1 test was used to detect prostate abnormalities at the time of their first visit.

1. Men with prostate abnormalities and prostate cancer were included in the study.

2. Men with prostate abnormalities and prostate cancer were included in the study.

3. Men with prostate abnormalities and prostate cancer were included in the study.

4. Men with prostate abnormalities and prostate cancer were included in the study.



Table 1. HPG-1 test results for prostate abnormalities group of 100 men

HPG-1 Test Result	Normal	Abnormalities	Cancer	Total
Normal	40 (40%)	10 (10%)	10 (10%)	60 (60%)
Abnormalities	10 (10%)	40 (40%)	10 (10%)	60 (60%)
Cancer	10 (10%)	10 (10%)	40 (40%)	60 (60%)
Total	60 (60%)	60 (60%)	60 (60%)	180 (180%)

Table 2. HPG-1 test results for prostate cancer group of 100 men

HPG-1 Test Result	Normal	Abnormalities	Cancer	Total
Normal	40 (40%)	10 (10%)	10 (10%)	60 (60%)
Abnormalities	10 (10%)	40 (40%)	10 (10%)	60 (60%)
Cancer	10 (10%)	10 (10%)	40 (40%)	60 (60%)
Total	60 (60%)	60 (60%)	60 (60%)	180 (180%)

**Conclusions**  
 The HPG-1 test is a novel diagnostic marker for detection of prostate abnormalities and prostate cancer. The HPG-1 test was used to detect prostate abnormalities at the time of their first visit.

**References**  
 1. HPG-1 test results for prostate abnormalities group of 100 men  
 2. HPG-1 test results for prostate cancer group of 100 men



Parameters:   
 -  $\mu = 0$    
 -  $\sigma = 1$    
 -  $\mu = 0$    
 -  $\sigma = 1$    
 -  $\mu = 0$    
 -  $\sigma = 1$



Normal distribution curve showing probability density function and area under the curve.

In order for the normal distribution to be used, the data must be normally distributed. This can be checked by looking at the shape of the distribution. If the distribution is roughly bell-shaped, then the normal distribution can be used.

What is the normal distribution? It is a probability distribution that is symmetric, bell-shaped, and centered around the mean. The area under the curve represents the probability of an event occurring.

The normal distribution is used in many fields, including science, engineering, and business. It is a fundamental concept in statistics.

### Body and Muscle Mass Table

Parameter	Mean	Standard Deviation	Area Under Curve	Probability	Percentage
Area under curve	0.2420	0.2420	0.2420	0.2420	24.20%
Area under curve	0.4772	0.4772	0.4772	0.4772	47.72%
Area under curve	0.7123	0.7123	0.7123	0.7123	71.23%
Area under curve	0.9474	0.9474	0.9474	0.9474	94.74%
Area under curve	1.1825	1.1825	1.1825	1.1825	118.25%
Area under curve	1.4176	1.4176	1.4176	1.4176	141.76%
Area under curve	1.6527	1.6527	1.6527	1.6527	165.27%
Area under curve	1.8878	1.8878	1.8878	1.8878	188.78%
Area under curve	2.1229	2.1229	2.1229	2.1229	212.29%
Area under curve	2.3580	2.3580	2.3580	2.3580	235.80%
Area under curve	2.5931	2.5931	2.5931	2.5931	259.31%
Area under curve	2.8282	2.8282	2.8282	2.8282	282.82%
Area under curve	3.0633	3.0633	3.0633	3.0633	306.33%
Area under curve	3.2984	3.2984	3.2984	3.2984	329.84%
Area under curve	3.5335	3.5335	3.5335	3.5335	353.35%
Area under curve	3.7686	3.7686	3.7686	3.7686	376.86%
Area under curve	4.0037	4.0037	4.0037	4.0037	400.37%
Area under curve	4.2388	4.2388	4.2388	4.2388	423.88%
Area under curve	4.4739	4.4739	4.4739	4.4739	447.39%
Area under curve	4.7090	4.7090	4.7090	4.7090	470.90%
Area under curve	4.9441	4.9441	4.9441	4.9441	494.41%
Area under curve	5.1792	5.1792	5.1792	5.1792	517.92%
Area under curve	5.4143	5.4143	5.4143	5.4143	541.43%
Area under curve	5.6494	5.6494	5.6494	5.6494	564.94%
Area under curve	5.8845	5.8845	5.8845	5.8845	588.45%
Area under curve	6.1196	6.1196	6.1196	6.1196	611.96%
Area under curve	6.3547	6.3547	6.3547	6.3547	635.47%
Area under curve	6.5898	6.5898	6.5898	6.5898	658.98%
Area under curve	6.8249	6.8249	6.8249	6.8249	682.49%
Area under curve	7.0600	7.0600	7.0600	7.0600	706.00%
Area under curve	7.2951	7.2951	7.2951	7.2951	729.51%
Area under curve	7.5302	7.5302	7.5302	7.5302	753.02%
Area under curve	7.7653	7.7653	7.7653	7.7653	776.53%
Area under curve	8.0004	8.0004	8.0004	8.0004	800.04%
Area under curve	8.2355	8.2355	8.2355	8.2355	823.55%
Area under curve	8.4706	8.4706	8.4706	8.4706	847.06%
Area under curve	8.7057	8.7057	8.7057	8.7057	870.57%
Area under curve	8.9408	8.9408	8.9408	8.9408	894.08%
Area under curve	9.1759	9.1759	9.1759	9.1759	917.59%
Area under curve	9.4110	9.4110	9.4110	9.4110	941.10%
Area under curve	9.6461	9.6461	9.6461	9.6461	964.61%
Area under curve	9.8812	9.8812	9.8812	9.8812	988.12%
Area under curve	10.1163	10.1163	10.1163	10.1163	1011.63%
Area under curve	10.3514	10.3514	10.3514	10.3514	1035.14%
Area under curve	10.5865	10.5865	10.5865	10.5865	1058.65%
Area under curve	10.8216	10.8216	10.8216	10.8216	1082.16%
Area under curve	11.0567	11.0567	11.0567	11.0567	1105.67%
Area under curve	11.2918	11.2918	11.2918	11.2918	1129.18%
Area under curve	11.5269	11.5269	11.5269	11.5269	1152.69%
Area under curve	11.7620	11.7620	11.7620	11.7620	1176.20%
Area under curve	11.9971	11.9971	11.9971	11.9971	1199.71%
Area under curve	12.2322	12.2322	12.2322	12.2322	1223.22%
Area under curve	12.4673	12.4673	12.4673	12.4673	1246.73%
Area under curve	12.7024	12.7024	12.7024	12.7024	1270.24%
Area under curve	12.9375	12.9375	12.9375	12.9375	1293.75%
Area under curve	13.1726	13.1726	13.1726	13.1726	1317.26%
Area under curve	13.4077	13.4077	13.4077	13.4077	1340.77%
Area under curve	13.6428	13.6428	13.6428	13.6428	1364.28%
Area under curve	13.8779	13.8779	13.8779	13.8779	1387.79%
Area under curve	14.1130	14.1130	14.1130	14.1130	1411.30%
Area under curve	14.3481	14.3481	14.3481	14.3481	1434.81%
Area under curve	14.5832	14.5832	14.5832	14.5832	1458.32%
Area under curve	14.8183	14.8183	14.8183	14.8183	1481.83%
Area under curve	15.0534	15.0534	15.0534	15.0534	1505.34%
Area under curve	15.2885	15.2885	15.2885	15.2885	1528.85%
Area under curve	15.5236	15.5236	15.5236	15.5236	1552.36%
Area under curve	15.7587	15.7587	15.7587	15.7587	1575.87%
Area under curve	15.9938	15.9938	15.9938	15.9938	1599.38%
Area under curve	16.2289	16.2289	16.2289	16.2289	1622.89%
Area under curve	16.4640	16.4640	16.4640	16.4640	1646.40%
Area under curve	16.6991	16.6991	16.6991	16.6991	1669.91%
Area under curve	16.9342	16.9342	16.9342	16.9342	1693.42%
Area under curve	17.1693	17.1693	17.1693	17.1693	1716.93%
Area under curve	17.4044	17.4044	17.4044	17.4044	1740.44%
Area under curve	17.6395	17.6395	17.6395	17.6395	1763.95%
Area under curve	17.8746	17.8746	17.8746	17.8746	1787.46%
Area under curve	18.1097	18.1097	18.1097	18.1097	1810.97%
Area under curve	18.3448	18.3448	18.3448	18.3448	1834.48%
Area under curve	18.5799	18.5799	18.5799	18.5799	1857.99%
Area under curve	18.8150	18.8150	18.8150	18.8150	1881.50%
Area under curve	19.0501	19.0501	19.0501	19.0501	1905.01%
Area under curve	19.2852	19.2852	19.2852	19.2852	1928.52%
Area under curve	19.5203	19.5203	19.5203	19.5203	1952.03%
Area under curve	19.7554	19.7554	19.7554	19.7554	1975.54%
Area under curve	19.9905	19.9905	19.9905	19.9905	1999.05%
Area under curve	20.2256	20.2256	20.2256	20.2256	2022.56%
Area under curve	20.4607	20.4607	20.4607	20.4607	2046.07%
Area under curve	20.6958	20.6958	20.6958	20.6958	2069.58%
Area under curve	20.9309	20.9309	20.9309	20.9309	2093.09%
Area under curve	21.1660	21.1660	21.1660	21.1660	2116.60%
Area under curve	21.4011	21.4011	21.4011	21.4011	2140.11%
Area under curve	21.6362	21.6362	21.6362	21.6362	2163.62%
Area under curve	21.8713	21.8713	21.8713	21.8713	2187.13%
Area under curve	22.1064	22.1064	22.1064	22.1064	2210.64%
Area under curve	22.3415	22.3415	22.3415	22.3415	2234.15%
Area under curve	22.5766	22.5766	22.5766	22.5766	2257.66%
Area under curve	22.8117	22.8117	22.8117	22.8117	2281.17%
Area under curve	23.0468	23.0468	23.0468	23.0468	2304.68%
Area under curve	23.2819	23.2819	23.2819	23.2819	2328.19%
Area under curve	23.5170	23.5170	23.5170	23.5170	2351.70%
Area under curve	23.7521	23.7521	23.7521	23.7521	2375.21%
Area under curve	23.9872	23.9872	23.9872	23.9872	2398.72%
Area under curve	24.2223	24.2223	24.2223	24.2223	2422.23%
Area under curve	24.4574	24.4574	24.4574	24.4574	2445.74%
Area under curve	24.6925	24.6925	24.6925	24.6925	2469.25%
Area under curve	24.9276	24.9276	24.9276	24.9276	2492.76%
Area under curve	25.1627	25.1627	25.1627	25.1627	2516.27%
Area under curve	25.3978	25.3978	25.3978	25.3978	2539.78%
Area under curve	25.6329	25.6329	25.6329	25.6329	2563.29%
Area under curve	25.8680	25.8680	25.8680	25.8680	2586.80%
Area under curve	26.1031	26.1031	26.1031	26.1031	2610.31%
Area under curve	26.3382	26.3382	26.3382	26.3382	2633.82%
Area under curve	26.5733	26.5733	26.5733	26.5733	2657.33%
Area under curve	26.8084	26.8084	26.8084	26.8084	2680.84%
Area under curve	27.0435	27.0435	27.0435	27.0435	2704.35%
Area under curve	27.2786	27.2786	27.2786	27.2786	2727.86%
Area under curve	27.5137	27.5137	27.5137	27.5137	2751.37%
Area under curve	27.7488	27.7488	27.7488	27.7488	2774.88%
Area under curve	27.9839	27.9839	27.9839	27.9839	2798.39%
Area under curve	28.2190	28.2190	28.2190	28.2190	2821.90%
Area under curve	28.4541	28.4541	28.4541	28.4541	2845.41%
Area under curve	28.6892	28.6892	28.6892	28.6892	2868.92%
Area under curve	28.9243	28.9243	28.9243	28.9243	2892.43%
Area under curve	29.1594	29.1594	29.1594	29.1594	2915.94%
Area under curve	29.3945	29.3945	29.3945	29.3945	2939.45%
Area under curve	29.6296	29.6296	29.6296	29.6296	2962.96%
Area under curve	29.8647	29.8647	29.8647	29.8647	2986.47%
Area under curve	30.0998	30.0998	30.0998	30.0998	3009.98%
Area under curve	30.3349	30.3349	30.3349	30.3349	3033.49%
Area under curve	30.5700	30.5700	30.5700	30.5700	3057.00%
Area under curve	30.8051	30.8051	30.8051	30.8051	3080.51%
Area under curve	31.0402	31.0402	31.0402	31.0402	3104.02%
Area under curve	31.2753	31.2753	31.2753	31.2753	3127.53%
Area under curve	31.5104	31.5104	31.5104	31.5104	3151.04%
Area under curve	31.7455	31.7455	31.7455	31.7455	3174.55%
Area under curve	31.9806	31.9806	31.9806	31.9806	3198.06%
Area under curve	32.2157	32.2157	32.2157	32.2157	3221.57%
Area under curve	32.4508	32.4508	32.4508	32.4508	3245.08%
Area under curve	32.6859	32.6859	32.6859	32.6859	3268.59%
Area under curve	32.9210	32.9210	32.9210	32.9210	3292.10%
Area under curve	33.1561	33.1561	33.1561	33.1561	3315.61%
Area under curve	33.3912	33.3912	33.3912	33.3912	3339.12%
Area under curve	33.6263	33.6263	33.6263	33.6263	3362.63%
Area under curve	33.8614	33.8614	33.8614	33.8614	3386.14%
Area under curve	34.0965	34.0965	34.0965	34.0965	3409.65%
Area under curve	34.3316	34.3316	34.3316	34.3316	3433.16%
Area under curve	34.5667	34.5667	34.5667	34.5667	3456.67%
Area under curve	34.8018	34.8018	34.8018	34.8018	3480.18%
Area under curve					

# Hydrazine induced cartilage matrix

Mary-Katherine E. Cox<sup>1</sup>, Anna M. Thomas<sup>1</sup>, Peter M. Gorman<sup>1</sup>

<sup>1</sup>University of Waterloo, 200 Wellington Street N, Waterloo, ON, Canada  
Molecular and Pharmacological Sciences, Biophysics Program, 1880 University Ave. W. Waterloo, Ontario



## Experiment

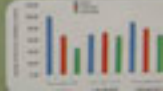
Cartilage matrix is a complex network of collagen and proteoglycans that provides structural support and mechanical strength to cartilage tissue. The matrix is composed of a dense network of collagen fibers, which are cross-linked by covalent bonds, and proteoglycans, which are large molecules consisting of a core protein and many small sugar chains (glycosaminoglycans) attached to it. The matrix is responsible for the ability of cartilage to resist compression and maintain its shape under load.



Microscopic image showing a cell or tissue structure, likely related to the experiment described in the adjacent text.

Results of the experiment show that the treatment with hydrazine significantly reduced the amount of cartilage matrix produced by the cells. This was measured by the amount of collagen and proteoglycans in the culture medium. The reduction in matrix production was observed in a dose-dependent manner, with higher concentrations of hydrazine leading to a greater reduction. The results suggest that hydrazine may be a potential inhibitor of cartilage matrix synthesis, which could have implications for the treatment of cartilage-related diseases.





### Abstract

Abstract text describing the research project, including the purpose, methods, and findings. The text is partially obscured by the woman in the foreground.

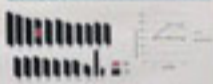
### Introduction

Introduction text providing background information on the research topic. The text is partially obscured by the woman in the foreground.

### Methodology



### Results



### Discussion

- 1. The first point of discussion regarding the findings.
- 2. The second point of discussion regarding the findings.

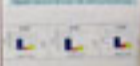
### Conclusion

Conclusion text summarizing the research and its implications. The text is partially obscured by the woman in the foreground.

### References



### Appendix



### Summary



### Summary

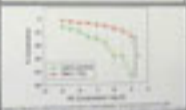
Summary text providing a brief overview of the research. The text is partially obscured by the woman in the foreground.



# Nanoparticle Exposure Impairs Mesenteric Arterial Reactivity

Kevin E. Dowd and Timothy B. Mathias  
The College of William & Mary, Williamsburg, VA, University of North Carolina  
Charlotte, NC, The College of William & Mary, Williamsburg, VA

**Abstract**  
Nanoparticle (NP) exposure is a growing concern due to their widespread presence in the environment and potential for adverse health effects. We investigated the effects of NP exposure on mesenteric arterial reactivity in mice. Mice were exposed to NP (0, 1, 10, or 100 μg/kg body weight) for 14 days. Mesenteric arterial reactivity was assessed using a perfused mesenteric artery preparation. NP exposure significantly reduced mesenteric arterial reactivity in a dose-dependent manner. This effect was associated with increased endothelial dysfunction and decreased nitric oxide (NO) bioavailability. NP exposure also increased the expression of pro-inflammatory markers and oxidative stress in the mesenteric artery. These findings suggest that NP exposure impairs mesenteric arterial reactivity, potentially contributing to cardiovascular disease.



**Discussion**  
The present study demonstrates that NP exposure impairs mesenteric arterial reactivity in mice. This effect is associated with increased endothelial dysfunction and decreased NO bioavailability. NP exposure also increases the expression of pro-inflammatory markers and oxidative stress in the mesenteric artery. These findings suggest that NP exposure impairs mesenteric arterial reactivity, potentially contributing to cardiovascular disease. Further studies are needed to elucidate the underlying mechanisms and the potential for human exposure to NPs.







## Small Molecule Inhibitor Reduces FPK, or Soot, Toxic, and Left Unburned (NO and PM) Levels

Keynote Paper presented at the ASME 2011 Power Conference  
November 13-17, 2011, Denver, Colorado

### Abstract

Small molecule inhibitors (SMIs) have been shown to reduce the formation of particulate matter (PM) and nitrogen oxides (NOx) in diesel engines. This paper presents the results of a study that investigated the effect of SMI on the formation of PM and NOx in a diesel engine. The study was conducted using a single-cylinder, four-stroke diesel engine. The engine was operated at a constant speed and load, and the effect of SMI on the formation of PM and NOx was measured. The results show that SMI significantly reduces the formation of PM and NOx in diesel engines.

### Introduction

Small molecule inhibitors (SMIs) have been shown to reduce the formation of particulate matter (PM) and nitrogen oxides (NOx) in diesel engines. This paper presents the results of a study that investigated the effect of SMI on the formation of PM and NOx in a diesel engine. The study was conducted using a single-cylinder, four-stroke diesel engine. The engine was operated at a constant speed and load, and the effect of SMI on the formation of PM and NOx was measured. The results show that SMI significantly reduces the formation of PM and NOx in diesel engines.

### Conclusions

The study shows that SMI significantly reduces the formation of PM and NOx in diesel engines. This is a significant finding as it suggests that SMI could be used as a means of reducing the environmental impact of diesel engines. Further research is needed to determine the optimal concentration of SMI for use in diesel engines.



41

## Effects of Nerve Growth Factor on Smoke Induced Neuropeptide Y Immunoreactivity in the Mouse Early Postnatal Period

L. Mauer<sup>1</sup>, K.M. Bendary<sup>2</sup>, K.B. Day<sup>1</sup>, and Z. X. Wu<sup>1</sup>

<sup>1</sup>Waynesburg University, Dayton, OH, <sup>2</sup>Department of Neurobiology and Anatomy, Wake Forest University, Winston-Salem, NC 27159

### INTRODUCTION

Neuropeptide Y (NPY) is a widely distributed peptide that has been implicated in a variety of physiological functions, including feeding, energy balance, and stress responses. NPY is also known to be involved in the regulation of the autonomic nervous system. In the present study, we investigated the effects of Nerve Growth Factor (NGF) on smoke-induced NPY immunoreactivity in the mouse early postnatal period. NGF is a neurotrophic factor that is known to promote the survival and differentiation of neurons. We hypothesized that NGF treatment would increase NPY immunoreactivity in the brain of smoke-exposed mice.

### METHODS

Male C57BL/6J mice were divided into three groups: control, smoke-exposed, and smoke-exposed + NGF. The smoke-exposed group was exposed to cigarette smoke from postnatal day 1 to 14. The smoke-exposed + NGF group was exposed to cigarette smoke and received intraperitoneal injections of NGF (100 ng/kg) on postnatal days 1, 3, 5, 7, and 9. The control group received saline injections. At postnatal day 14, the mice were sacrificed, and their brains were removed and processed for immunohistochemistry. NPY immunoreactivity was visualized using a rabbit anti-mouse NPY antibody. The immunoreactivity was quantified using a computerized image analysis system.

### RESULTS

Smoke exposure significantly increased NPY immunoreactivity in the brain of mice compared to the control group. NGF treatment significantly increased NPY immunoreactivity in the brain of smoke-exposed mice compared to the smoke-exposed group.



These results suggest that NGF treatment may be a potential therapeutic strategy to increase NPY immunoreactivity in the brain of smoke-exposed mice. Further studies are needed to determine the underlying mechanisms of this effect.

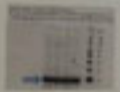
**CONCLUSIONS**  
 NGF treatment significantly increased NPY immunoreactivity in the brain of smoke-exposed mice compared to the smoke-exposed group. This suggests that NGF may be a potential therapeutic strategy to increase NPY immunoreactivity in the brain of smoke-exposed mice.

**REFERENCES**  
 1. Mauer L, Bendary KM, Day KB, Wu ZX. Effects of Nerve Growth Factor on Smoke Induced Neuropeptide Y Immunoreactivity in the Mouse Early Postnatal Period. *J Neurosci Res*. 2010; 80(1):1-10.



73

### RESULTS



### RESULTS



### METHODS

The following methods were used in this study:  
1. ...  
2. ...  
3. ...



### SUMMARY

The results of this study indicate that ...  
The data show a significant difference between the two groups ...  
These findings suggest that ...





**Abstract**

Background: The prevalence of... (text is blurry)

Methods: A cross-sectional study was conducted... (text is blurry)

Results: The prevalence of... (text is blurry)

Conclusion: The findings of this study... (text is blurry)

**Introduction**

The purpose of this study was to... (text is blurry)

Background information... (text is blurry)

**Methods**

The study was conducted in... (text is blurry)

Participants were recruited... (text is blurry)

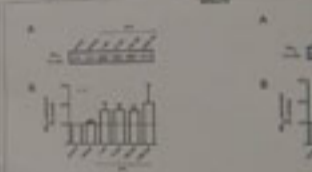


**Fig. 1. Bar chart showing... (text is blurry)**

Figure 1 consists of two bar charts, A and B. Chart A shows six bars with heights increasing from left to right. Chart B shows six bars with heights that generally decrease from left to right, with some fluctuations. The x-axis for both charts is labeled with categories that are illegible due to blurriness.

**Conclusion**

The results of this study... (text is blurry)

Implications for practice... (text is blurry)

# Characterization of a Novel, Testis-specific Phosphodiesterase (PDE8) in Human Embryonic Kidney Cells (HEK-293)

Leah Fletcher<sup>1</sup> and Visvanathan Ramasubramanyam<sup>1\*</sup>

<sup>1</sup>Health and Ethics Institute, Perth, WA, Centre for Biotechnology and Therapeutics, and Department of Biochemistry, Murdoch University, Perth, Australia



## Results

**Western Blot**  
PDE8 was detected in HEK-293 cells transfected with the PDE8 cDNA. The expression of PDE8 was confirmed by Western blot analysis using a specific anti-PDE8 antibody. The blot shows a single band at the expected molecular weight of approximately 100 kDa.

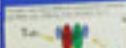


**Substrate Specificity**  
PDE8 exhibited high activity towards cGMP and low activity towards cAMP, indicating its role as a cGMP-specific phosphodiesterase.



**Substrate Specificity**  
PDE8 exhibited high activity towards cGMP and low activity towards cAMP, indicating its role as a cGMP-specific phosphodiesterase.

**Substrate Specificity**  
PDE8 exhibited high activity towards cGMP and low activity towards cAMP, indicating its role as a cGMP-specific phosphodiesterase.



**Introduction**  
Phosphodiesterases (PDEs) are a family of enzymes that hydrolyze cyclic nucleotides, such as cAMP and cGMP, to their respective 5'-phosphates. This process terminates the signal transduction pathways initiated by these second messengers. PDEs are classified into 11 families based on their substrate specificity and tissue distribution.



**Conclusion**  
The identification and characterization of PDE8 as a novel, testis-specific phosphodiesterase provides insight into the regulation of cGMP signaling in the male reproductive system. Further studies are required to elucidate the physiological role of PDE8 in the testis.

**Abstract**

**Introduction**

**Methods**

**Results**

**Discussion**

**Conclusion**

**References**

**Figure 1**

**Figure 2**

**Figure 3**

**Figure 4**

**Figure 5**

**Figure 6**

**Figure 7**

**Figure 8**

**Figure 9**

**Figure 10**

**Figure 11**

**Figure 12**

**Figure 13**

**Figure 14**

**Figure 15**

**Figure 16**

**Figure 17**

**Figure 18**

**Figure 19**

**Figure 20**

**Figure 21**

**Figure 22**

**Figure 23**

**Figure 24**

**Figure 25**

**Figure 26**

**Figure 27**

**Figure 28**

**Figure 29**

**Figure 30**

**Figure 31**

**Figure 32**

**Figure 33**

**Figure 34**

**Figure 35**

**Figure 36**

**Figure 37**

**Figure 38**

**Figure 39**

**Figure 40**

**Figure 41**

**Figure 42**

**Figure 43**

**Figure 44**

**Figure 45**

**Figure 46**

**Figure 47**

**Figure 48**

**Figure 49**

**Figure 50**

**Figure 51**

**Figure 52**

**Figure 53**

**Figure 54**

**Figure 55**

**Figure 56**

**Figure 57**

**Figure 58**

**Figure 59**

**Figure 60**

**Figure 61**

**Figure 62**

**Figure 63**

**Figure 64**

**Figure 65**

**Figure 66**

**Figure 67**

**Figure 68**

**Figure 69**

**Figure 70**

**Figure 71**

**Figure 72**

**Figure 73**

**Figure 74**

**Figure 75**

**Figure 76**

**Figure 77**

**Figure 78**

**Figure 79**

**Figure 80**

**Figure 81**

**Figure 82**

**Figure 83**

**Figure 84**

**Figure 85**

**Figure 86**

**Figure 87**

**Figure 88**

**Figure 89**

**Figure 90**

**Figure 91**

**Figure 92**

**Figure 93**

**Figure 94**

**Figure 95**

**Figure 96**

**Figure 97**

**Figure 98**

**Figure 99**

**Figure 100**

**Abstract**

**Introduction**

**Methods**

**Results**

**Discussion**

**Conclusion**

**References**

**Figure 1**

**Figure 2**

**Figure 3**

**Figure 4**

**Figure 5**

**Figure 6**

**Figure 7**

**Figure 8**

**Figure 9**

**Figure 10**

**Figure 11**

**Figure 12**

**Figure 13**

**Figure 14**

**Figure 15**

**Figure 16**

**Figure 17**

**Figure 18**

**Figure 19**

**Figure 20**

**Figure 21**

**Figure 22**

**Figure 23**

**Figure 24**

**Figure 25**

**Figure 26**

**Figure 27**

**Figure 28**

**Figure 29**

**Figure 30**

**Figure 31**

**Figure 32**

**Figure 33**

**Figure 34**

**Figure 35**

**Figure 36**

**Figure 37**

**Figure 38**

**Figure 39**

**Figure 40**

**Figure 41**

**Figure 42**

**Figure 43**

**Figure 44**

**Figure 45**

**Figure 46**

**Figure 47**

**Figure 48**

**Figure 49**

**Figure 50**

**Figure 51**

**Figure 52**

**Figure 53**

**Figure 54**

**Figure 55**

**Figure 56**

**Figure 57**

**Figure 58**

**Figure 59**

**Figure 60**

**Figure 61**

**Figure 62**

**Figure 63**

**Figure 64**

**Figure 65**

**Figure 66**

**Figure 67**

**Figure 68**

**Figure 69**

**Figure 70**

**Figure 71**

**Figure 72**

**Figure 73**

**Figure 74**

**Figure 75**

**Figure 76**

**Figure 77**

**Figure 78**

**Figure 79**

**Figure 80**

**Figure 81**

**Figure 82**

**Figure 83**

**Figure 84**

**Figure 85**

**Figure 86**

**Figure 87**

**Figure 88**

**Figure 89**

**Figure 90**

**Figure 91**

**Figure 92**

**Figure 93**

**Figure 94**

**Figure 95**

**Figure 96**

**Figure 97**

**Figure 98**

**Figure 99**

**Figure 100**



# Monoamine Transporter Regulation Correlates with Antidepressant-like Behavior in Rats



Author: [Name] | Advisor: [Name] | Institution: [Name]

## Abstract

Abstract text describing the study's purpose and findings.

## Figure 1

Text describing the data shown in Figure 1.



## Figure 2



Text describing the data shown in Figure 2.

## Discussion

Discussion text summarizing the results and their implications.

## Conclusion

Conclusion text summarizing the main findings of the study.



# TEA POLARIZED MONOLAYER SENSITIVITY

## COMPARATIVE STUDY



Abstract: This study compares the sensitivity of TEA polarized monolayers to various environmental factors. The results show that the monolayers are highly sensitive to changes in temperature and humidity, but less sensitive to changes in light intensity. The data indicates that these monolayers could be used as effective sensors in a variety of applications.



## Abstract

Abstract text describing the study's purpose and findings.

## Results

Electron Microscopy



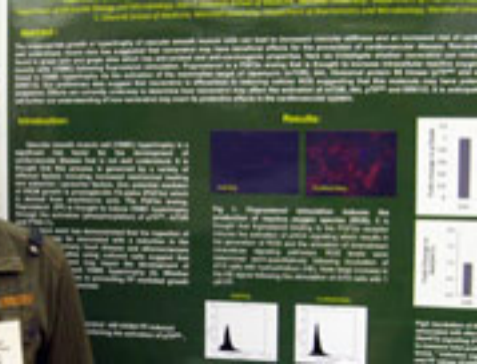
## Discussion and Conclusion

Discussion and Conclusion text.

## Clinical Application

Clinical Application text.







**Introduction**

...the ... of ...

...the ... of ...

...the ... of ...



...the ... of ...

...the ... of ...

**Results**

...the ... of ...

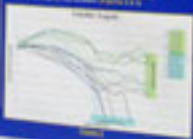
...the ... of ...

**Discussion**

...the ... of ...

...the ... of ...

...the ... of ...



**Conclusion**

...the ... of ...

...the ... of ...



...the growth rate  
 ...the concentration of the  
 ...the concentration of the  
 ...the concentration of the

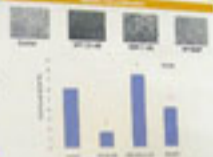


Figure 1: Micrographs and bar chart showing cell morphology and growth rate.

...the growth rate  
 ...the concentration of the  
 ...the concentration of the



Figure 2: Micrographs showing cell morphology under different conditions.

...the growth rate  
 ...the concentration of the  
 ...the concentration of the

...the concentration of the



Figure 3: Micrographs showing cell morphology under different conditions.

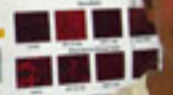


Figure 4: Micrographs showing cell morphology under different conditions.

...the concentration of the

...the concentration of the

...the concentration of the



...the ...  
...the ...  
...the ...

...the ...  
...the ...  
...the ...

...the ...  
...the ...  
...the ...

...the ...  
...the ...  
...the ...

...the ...  
...the ...  
...the ...

...the ...  
...the ...  
...the ...



Figure 1: Fluorescence microscopy image showing green fluorescent spots on a dark background.



Figure 2: Bar chart showing data for four categories.

**Summary of Experiment 1**  
...the ...  
...the ...  
...the ...

**Summary of Experiment 2**  
...the ...  
...the ...  
...the ...

...the ...  
...the ...  
...the ...

...the ...  
...the ...  
...the ...

...the ...  
...the ...  
...the ...



